^{13}C Magic Angle Spinning NMR Analysis and Quantum Chemical Modeling of the Bathochromic Shift of Astaxanthin in α-Crustacyanin, the Blue Carotenoprotein Complex in the Carapace of the Lobster *Homarus gammarus*†

Roland J. Weesie,‡,§,||,⊥ Frans Jos H. M. Jansen,‡ Jean Claude Merlin,|| Johan Lugtenburg,‡ George Britton,§ and Huub J. M. de Groot*,‡

Leiden Institute of Chemistry, Gorlaeus Laboratories, Leiden University, P.O. Box 9502, 2300 RA Leiden, The Netherlands, School of Biological Sciences, University of Liverpool, Crown Street, Liverpool L69 7ZB, United Kingdom, and Laboratoire de Spectrochimie Infrarouge et Raman, CNRS LP 2631, Université des Sciences et Technologies de Lille, Bât. C5, 59655 Villeneuve d'Ascq Cedex, France

Received December 30, 1996; Revised Manuscript Received April 3, 1997⊗

ABSTRACT: Selective isotope enrichment, ^{13}C magic angle spinning (MAS) NMR, and semiempirical quantum chemical modeling, have been used to analyze ligand−protein interactions associated with the bathochromic shift of astaxanthin in α-crustacyanin, the blue carotenoprotein complex from the carapace of the lobster *Homarus gammarus*. Spectra of α-crustacyanin were obtained after reconstitution with astaxanthins labeled with ^{13}C at positions 4,4′, 12,12′, 13,13′, or 20,20′. The data reveal substantial downfield shifts of 4.9 and 7.0 ppm at positions 12 and 12′ in the complex, respectively. In contrast, at the 13 and 13′ positions, small upfield shifts of 1.9 ppm were observed upon binding to the protein. These data are in line with previously obtained results for positions 14,14′ (3.9 and 6.8 ppm downfield) and 15,15′ (0.6 ppm upfield) and confirm the unequal perturbation of both halves after binding of the chromophore. However, these results also show that the main perturbation is of symmetrical origin, since the chemical shift differences exhibit a similar pattern in both halves of the astaxanthin molecule. A small downfield shift of 2.4 ppm was detected for the 4 and 4′ positions. Finally, the 20,20′ methyl groups are shifted 0.4 ppm upfield by the protein. The full data set provides convincing evidence that charge polarization is of importance for the bathochromic shift. The NMR shifts are compared with calculated charge densities for astaxanthin subjected to variations in protonation states of the ring-functional groups, as models of ligand−protein interactions. Taking into account the color shift and other available optical data, the current model for the mechanisms of interaction with the protein was refined. The results point toward a mechanism in which the astaxanthin is charged and subject to strong electrostatic polarizations originating from both keto groups, most likely a double protonation.

Carotenoids are the most widespread class of pigments in both plants and animals. They are responsible for many natural yellow, orange, or red colors. In addition, when carotenoids are associated with proteins, these colors can be modified to green, purple, or blue by the formation of carotenoid−protein complexes. A well-known example of this phenomenon is provided by the lobster *Homarus gammarus*, which in its natural state is deep blue, due to the presence of the carotenoprotein α-crustacyanin. Heat causes the lobster to change color from blue to red, since at high temperature, the crustacyanin denatures and astaxanthin is liberated. The crustacyanins are good models for studying one particular class of ligand−protein interactions that play such fundamental roles in many biological and biochemical processes; for this, the molecular mechanisms behind the large bathochromic shift and the nature of the corresponding protein−chromophore interactions need to be elucidated.

The natural α-crustacyanin is a water-soluble 320 kDa carotenoprotein complex which consists of eight β-crustacyanin dimers (41 kDa), each of which contains two polypeptide chains and two astaxanthin molecules. The absorption maximum shifts from ∼480 to 632 nm when the astaxanthin is bound in the hexadecameric α-crustacyanin complex. The carotenoids are noncovalently bound to the apoprotein in a stoichiometric way. There are five electrophoretically distinct monomer subunits, termed A_1, A_2, A_3, C_1, and C_2. The A subunits move toward the anode during gel electrophoresis, and the C particles migrate toward the cathode (Quarmby et al., 1977). The monomeric subunits A_1, C_1, and C_2 have a molecular mass of ca. 21×10^3 Da, while each of the A_2 and A_3 monomers has a molecular mass of approximately 19×10^3 Da (Quarmby et al., 1977; Zagalsky, 1982). There appears to be a preference for β-crustacyanin dimers made from one 19 kDa and one 21 kDa subunit, in combination with two astaxanthin molecules. From the six preferred β-crustacyanin species that can be formed in this way, the combination of the A_2 and C_1

† This research was supported by SCIENCE contract SC1-CT92-0813 of the European Commission and by the Netherlands Foundation for Chemical Research (SON), financed by the Netherlands Organization for Scientific Research (NWO). R.J.W. acknowledges a short term fellowship from the European Molecular Biology Organisation (EMBO).

‡ Leiden University.

§ University of Liverpool.

|| Université des Sciences of Technologies de Lille.

⊥ Present address: Laboratoire d'Analyse Isotopique et Electrochimique de Métabolismes, Université de Nantes, B.P. 92208, 2 rue de la Houssinière, 44322 Nantes Cedex 03, France.

⊗ Abstract published in *Advance ACS Abstracts,* May 15, 1997.

S0006-2960(96)03198-4 CCC: $14.00

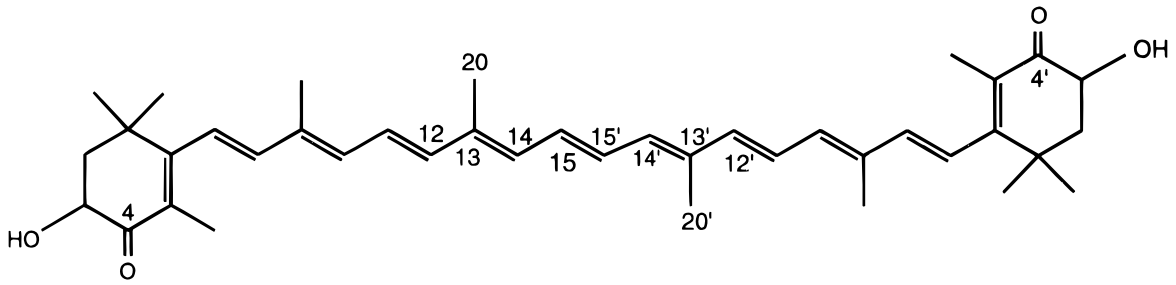

FIGURE 1: Structure of astaxanthin (3,3′-dihydroxy-β,β-carotene-4,4′-dione). The numbers indicate the positions that were labeled for the CP/MAS NMR studies of the α-crustacyanin complex.

subunits is the most commonly found (Quarmby et al., 1977). Free β-crustacyanin dimers have a λ_{max}[1] of 585 nm and can be formed in solution by dialyzing α-crustacyanin against 5 L of distilled water containing 1 mL of 1.5 M Tris-HCl (pH 8.8).

It is generally accepted that complexation of two or more astaxanthins in the crustacyanins leads to no increase of the optical transition moment (Buchwald & Jencks, 1968b). It is thought that highly localized and specific interactions are responsible for the large red shift of the astaxanthin in the complex, but the precise mechanisms that could account for such a large color shift are still a matter of debate. First, Buchwald and Jencks (1968b) proposed a distortion mechanism in which the spectral shift would arise from strain in the double bonds of the conjugated backbone of the carotenoid [for a review see Zagalsky et al. (1990)]. Salares et al. (1979), however, favored a polarization mechanism and opposed the distortion mechanism on the basis of their studies of the crustacyanins by Raman spectroscopy.

Recently, the first direct experimental evidence for a charge redistribution mechanism contributing to the bathochromic shift of the chromophore in α-crustacyanin was obtained by means of site-specific isotope enrichment of astaxanthin with ^{13}C at the 14,14′ and 15,15′ positions (Weesie et al., 1995). To achieve this, selectively labeled [14,14′-$^{13}C_2$]- and [15,15′-$^{13}C_2$]astaxanthin were synthesized, reconstituted into the protein, and studied by ^{13}C CP/MAS NMR. Although the first NMR data only probed a small part of the polyene chain, they clearly demonstrated that the effect of protein binding is not identical in both halves of the astaxanthin molecule (Weesie et al., 1995). However, the first limited data set did not reveal any information about the nature of the main perturbation. This requires knowledge of the chemical shifts at other sites along the polyene chain. Building upon the first successes with labeling and CP/MAS NMR, we are now engaged in a systematic study aimed at a detailed characterization of the ligand−protein interactions in the naturally occurring α-crustacyanin. Here, we present the ^{13}C CP/MAS NMR spectra of the blue hexadecamer after reconstitution with astaxanthins specifically labeled with ^{13}C at the 12,12′ or 13,13′ positions, adjacent to the 14,14′ and 15,15′ sites that were studied earlier. In addition, two important binding motifs, the central methyl groups and the ring keto groups, are probed with 20,20′-$^{13}C_2$ and 4,4′-$^{13}C_2$ labeling in the astaxanthin. The positions of labeling are indicated in the scheme in Figure 1.

The NMR data are compared with the results of quantum chemical calculations of charge density differences for astaxanthins subject to strong electrostatic perturbations. On the basis of this comparison and the calculated spectral shifts, the current model for the protein−chromophore interactions in the α-crustacyanin complex can be refined.

MATERIALS AND METHODS

α-Crustacyanin was extracted from finely ground lobster carapace and purified by anion-exchange and gel-filtration chromatography (Zagalsky, 1985). The extraction and purification stages were all carried out at 4 °C, and the pH was maintained between 6.5 and 7.5. The purity of the α-crustacyanin preparation was measured by the ratio of absorbance at 632 nm to protein absorbance at 280 nm, and the total amount of α-crustacyanin present in the protein solution was determined from the absorbance at 632 nm. A molar absorption coefficient ϵ of 1.25×10^5 M^{-1} cm^{-1} was used (Zagalsky et al., 1983).

The reconstitution procedure was based on a method described earlier (Zagalsky, 1985). All stages of reconstitution were carried out at 0 °C in a ground glass stoppered tube. The solvents and buffers added during the procedure were first cooled to 0 °C. To α-crustacyanin in 50 mM sodium phosphate buffer at pH 7.0 (2 mL, containing up to 3 mg of protein), was quickly added acetone with much stirring, followed by the addition of diethyl ether (10 mL). The tube was inverted three times, and the orange ether layer, containing extracted astaxanthin, was pipetted off until no more carotenoid could be extracted. Any remaining ether was quickly removed with a gentle flow of nitrogen, and the protein solution was made up to 2 mL again with 50 mM sodium phosphate buffer (pH 7.0) if necessary. The acetone/ether extraction was repeated twice more, removing virtually all the astaxanthin and leaving an almost colorless apoprotein preparation. Finally, all the volatile solvent remaining was removed with a nitrogen flow in 5−10 min.

A 25% molar excess of the labeled astaxanthin in acetone (1.25 mL) was quickly added to the apoprotein preparation, with much stirring, followed immediately by the addition of 50 mM sodium phosphate buffer at pH 7.0 (10 mL). This mixture was dialyzed for 18 h against 5 L of the same buffer. The reconstituted complex was shown to be identical to the natural α-crustacyanin as judged by the optical, resonance Raman, and ^{13}C CP/MAS NMR spectra of both species (Weesie et al., 1995).

The ^{13}C-labeled astaxanthins were prepared by organic synthesis which is described elsewhere (Jansen et al., 1994). Approximately 20 mg of α-crustacyanin reconstituted with ^{13}C-labeled astaxanthin was used to record each ^{13}C CP/MAS NMR spectrum. The NMR samples were first concentrated by means of 100 kDa Macrosep centrifugal concentrators with a volume of 20 mL (Filtron Technology Corp., Northborough, MA) to a volume of approximately 2 mL and

[1] Abbreviations: AM1, Austin method 1; CP, cross-polarization; ΔH, heat of formation; MAS, magic angle spinning; NMR, nuclear magnetic resonance; PM3, parametrization method 3; TMS, tetramethylsilane; λ_{max}, wavelength of maximum optical absorption.

then with 50 kDa Microsep centrifugal concentrators with a volume of 3.5 mL to give a final volume of around 100 μL. This concentration procedure yielded very dense protein solutions with a protein concentration of 200 mg/mL. Optical absorption spectra of aliquots of the final protein solutions, which were taken just before and after the NMR experiments, were found to be identical to the spectra of the starting solutions. This confirmed that no denaturation had occurred during the concentration or recording of the NMR spectrum.

Low-temperature 100 MHz ^{13}C CP/MAS NMR experiments on the α-crustacyanin carotenoprotein complex were performed with a Bruker MSL-400 NMR spectrometer equipped with a 4 mm MAS probe (Bruker, Karlsruhe, Germany). The spinning rate around the magic angle was measured by means of an optical detection system and was kept stable at 5.00 ± 0.01 or 6.00 ± 0.01 kHz with a home-built spinning speed controller (de Groot et al., 1988).

The spectra were accumulated in 1K channels with continuous ^{1}H decoupling during acquisition. The 90° pulse lengths for the ^{1}H and ^{13}C were 6−7 μs, the cross-polarization time was 1 ms, the recycle delay 1 s, and the sweep width 50 kHz. Chemical shifts are referenced to TMS, and all spectra were recorded with a dead time of 10 μs. The protein data were collected with a sample temperature T of ∼230 ± 5 K, calculated from the empirical relationship $T \sim 0.86T_B + 50$ K (H. Förster and A. C. Kolbert, unpublished results). Here, T_B is the temperature of the bearing gas, which was measured with a thermocouple just in front of the gas inlet of the spinner assembly.

The modeling of NMR shift differences and optical absorption energies was performed with a combination of classical molecular mechanics and semiempirical quantum chemical methods. The initial configurations were set up with standard geometrical parameters that were subsequently optimized using the PC MODEL (version 3.2) program which makes use of an MMX force field (Gajewski & Gilbert, 19XX), including the π-VESCF calculations. The refined structures were then used as input data for AM1 or PM3 geometry optimization using the MOPAC 93 program on an Indy Silicon Graphics workstation or the HYPERCHEM package (version 4.5) on a Pentium microcomputer. The calculation of the astaxanthin geometry was progressively carried out by successively releasing the internal coordinates. The final energy minimum was obtained by simultaneous relaxation of all the geometrical parameters. The calculations on electrostatically perturbed or charged astaxanthin-like structures were performed using the geometrical parameters of the optimized astaxanthin molecule as input data. Bond lengths, bond angles, and torsional angles, as well as the electronic charge density for each atom, were evaluated after structure optimization. Electronic spectra were produced by single excited configuration interaction calculations performed on the optimized structures. Excitation energies for the excited states, together with the transition dipole moment and intensities for each possible excitation, were thus obtained.

RESULTS

CP/MAS NMR Analysis of α-Crustacyanin with ^{13}C Labels in the Astaxanthin. It has been shown in the past that the CP/MAS technique in conjunction with selective isotope enrichment allows the investigation of ligand−protein interactions at atomic resolution for essentially unperturbed and unmodified ligand−protein complexes, which is a prerequisite for the elucidation of specific binding and interaction mechanisms [see e.g. Van Liemt et al. (1995) and Smith et al. (1990)]. In these studies, individual carbons must be labeled with NMR isotopes by total synthesis of ligands. The initial choice of the positions of the ^{13}C labels in the astaxanthin chromophore was guided by the results that had already been obtained with other techniques. In particular, resonance Raman experiments suggested that the central part of the astaxanthin chromophore is in a relatively planar conformation and only slightly distorted, while reconstitution experiments with the demethylated astaxanthins (Warburton, 1986) seemed to favor a more twisted conformation (Salares et al., 1979). In view of these conflicting opinions, we originally decided to start with the investigation of the central part of the chromophore and to study the effect on the chemical shift after protein binding in this particular region. The first results, with [14,14′-$^{13}C_2$]- and [15,15′-$^{13}C_2$]astaxanthins, were reported in a preliminary communication (Weesie et al., 1995). Here, we extend this study and include the carbon positions 12,12′, 13,13′, and 20,20′ in the central part of the polyene chain and positions 4,4′ in the rings to probe the keto groups that are crucial for the binding of the astaxanthin.

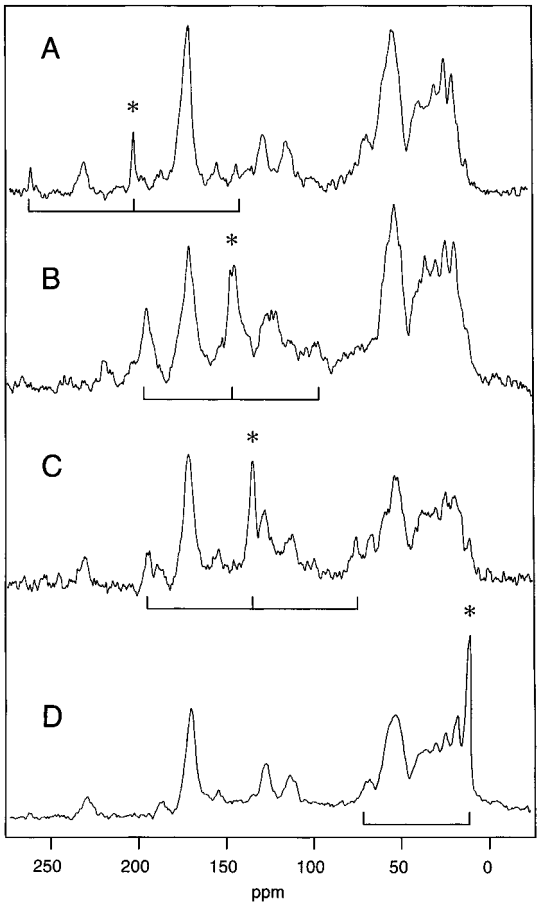

FIGURE 2: ^{13}C CP/MAS NMR data for α-crustacyanin, labeled with [4,4′-$^{13}C_2$]astaxanthin (A), [12,12′-$^{13}C_2$]astaxanthin (B), [13,13′-$^{13}C_2$]astaxanthin (C), and [20,20′-$^{13}C_2$]astaxanthin (D). The center band signals from the labels are indicated with ∗. The square brackets indicate the positions of the MAS side bands relative to the center bands. To avoid overlap between signals from center bands and side bands, relatively high spinning speeds of 5.00 kHz (B) and 6.00 kHz (A, C, D) were used.

In Figure 2 are shown the ^{13}C CP/MAS NMR spectra of α-crustacyanin reconstituted with labeled astaxanthin. Traces

Table 1: Isotropic Chemical Shifts σ_i and Reconstitution Shifts $\Delta\sigma_i$ for the Labels in the Pure Solid Astaxanthin and in the α-Crustacyanin[a]

labels	$\sigma_{i\,(ppm)}$ astaxanthin	α-crustacyanin	$\Delta\sigma_i$ (ppm)
4,4′	201.0	203.4	2.4
12,12′	140.2	145.1, 147.2	4.9, 7.0
13,13′	137.1	135.2	−1.9
14,14′[b]	134.1	138.0, 140.9	3.9, 6.8
15,15′[b]	130.1	129.5	−0.6
20,20′	11.5	11.1	−0.4

[a] Estimated errors are ±0.2 ppm. [b] Data from Weesie et al. (1995).

A, C, and D, for the 4,4′-$^{13}C_2$, 13,13′-$^{13}C_2$, and 20,20′-$^{13}C_2$ labels, were recorded at a rotation frequency $\omega_r/2\pi$ of 6 kHz, while spectrum B, for the 12,12′-$^{13}C_2$ sample, was recorded at a rotation frequency $\omega_r/2\pi$ of 5 kHz. The major part of the NMR response is from the natural abundance ^{13}C and contains several characteristic features. Thus, the C═O resonances of the peptide groups give a signal at a σ_i of ∼172 ppm. Less intense signals at *ca*. 128 ppm can be assigned to the aromatic and olefinic carbon atoms in the protein, while the aliphatic carbons are responsible for signals in the region between 0 and 80 ppm. In the spectra in Figure 2, which are from crustacyanins that are reconstituted with ^{13}C-labeled astaxanthins, additional resonance signals with corresponding side bands are observed from the ^{13}C labels. In Figure 2, the center band responses from the labels are indicated with asterisks.

The isotropic ^{13}C shifts σ_i of the label signals are presented in Table 1. In addition, CP/MAS spectra of the pure labeled astaxanthins were collected and the isotropic shifts of the labels are included in Table 1. The shift differences induced by binding, $\Delta\sigma_i$, are largest for [12,12′-$^{13}C_2$]astaxanthin and are comparable to those obtained for [14,14′-$^{13}C_2$]astaxanthin-reconstituted material (Weesie et al., 1995). A single resonance signal is observed for the 12,12′-$^{13}C_2$ response of the pure solid, but this is split when the astaxanthin is bound into the protein complex, yielding the two values for σ_i reported in Table 1. In the ^{13}C CP/MAS NMR spectrum of α-crustacyanin reconstituted with [13,13′-$^{13}C_2$]astaxanthin, a single resonance signal at 135.2 ppm is seen for the ^{13}C labels and the upfield shift due to binding to the protein $\Delta\sigma_i$ = 1.9 ppm.

Since reconstitution studies revealed that the presence of the 20,20′ methyl groups is critical for complexation and binding, [20,20′-$^{13}C_2$]astaxanthin was also synthesized and investigated in the α-crustacyanin. These labels also give rise to a single response with a σ_i of 11.1 ppm, almost equal to the σ_i of 11.4 ppm observed for the crystalline astaxanthin. In order to obtain an NMR assay of the protein−chromophore interactions for the other predominant binding motif, the ring keto groups, we decided to synthesize astaxanthin labeled at the 4,4′ positions and to record the ^{13}C CP/MAS NMR spectrum of α-crustacyanin reconstituted with this [4,4′-$^{13}C_2$]astaxanthin. A response from the labels was observed in a single resonance with a σ_i of 203.4 ppm.

The intensity of the 4,4′-$^{13}C_2$ resonance signals is weaker than that for the other ^{13}C resonances. To check whether the C-4,4′ signals exhibit any temperature dependence, spectra were collected at different temperatures, varying from a *T* of 120 K to a *T* of 250 K, just below the freezing point of the α-crustacyanin complex, but no temperature dependence was found. At this point, it is not clear what is responsible for the significantly lower signal intensity of the C-4,4′ resonance signals. It can at least partly be explained by considering that the carbons at positions 4,4′ are quaternary carbons. Since the magnetization in a ^{13}C CP/MAS NMR experiment is transferred from the ^1H spins to the ^{13}C spins, a short C−H distance may facilitate the magnetization transfer and result in stronger ^{13}C signals.

Semiempirical Modeling of Astaxanthin−Protein Interactions Acting at the Rings. On the basis of the optical spectroscopy data, it was concluded that the astaxanthin in the complex is spectroscopically a monomer (Buchwald & Jencks, 1968b; Merlin & Delé-Dubois, 1986), while the NMR data point toward a mechanism in which additional polarizations of the chromophore are induced by binding to the protein. To interpret the NMR results and to correlate these with other experimental data already available in the literature, semiempirical quantum chemical calculations were performed for free astaxanthin and for a single carotenoid molecule exposed to highly localized and specific interactions with pronounced charge effects on the polyene system.

The semiempirical quantum chemical modeling proceeds in two steps. In a first step, the color and charge delocalization are calculated for model structures that are different from astaxanthin in the sense that they are subject to strong highly localized interactions or modifications that affect the keto or hydroxy groups. In Table 2, the chemical structures of electrostatically perturbed or charged forms of astaxanthin are shown together with their calculated electronic transition wavelengths λ_{max}. These structural modifications involve either a protonation of one or both of the β-ring keto groups (structures **II**−**IV**), a deprotonation of both hydroxyl groups (structure **VII**), or an internal migration of protons from the hydroxyl groups to the keto groups (structure **I**). The common denominator in these models is the fact that the polyene system is polarized by additional Coulombic interactions originating from the ring end groups. The charge densities of the bare modified or charged structures provide a reliable fast criterium for assessing the validity of the structure as a model for protein-bound astaxanthin, leading to a first selection of the model structures.

Although charging is easily achieved in the virtual reality of the computer, charged structures are difficult to maintain within a protein environment and require the presence of water or counterions for a good stabilization. Generally, the electron transfer between the charged model and stabilizing groups is small, but the mutual polarization effects associated with the stabilization can reduce the delocalization of the charge over the structure considerably, which will be accompanied by a reduction of the optical gap and the color shift. A prominent example of the stabilization of a charged chromophore and the associated mutual polarization effects can be found in the retinal proteins, which contain fully protonated Schiff bases and have been studied extensively with MAS NMR. Here, it is thought that the local proton chemical potential in the protein is raised and stabilized by a complex counterion, involving water supported by protic amino acid side chains (de Groot et al., 1989, 1990). In addition, charged groups in the protein can contribute directly to the tuning of the polarization and the color (Smith et al., 1990).

Along the same lines, a protonated keto group and the associated positive charge, delocalized into the polyene chain, can also be stabilized with a water molecule in a hydrogen bonding position (structure **IV**) or a monovalent counterion

Table 2: Overview of the Calculated λ_{max} for Different Forms of Astaxanthin, Neutral or Charged by Various Mechanisms, Involving Intramolecular Hydrogen Migration, Protonation, or Deprotonation of the Ring Keto and Hydroxy Groups[c]

	Structure	charge	λ_{max} (nm)
	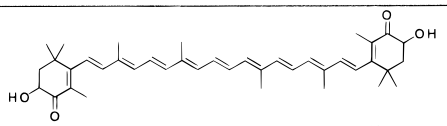	0	441[a] 432[b]
I	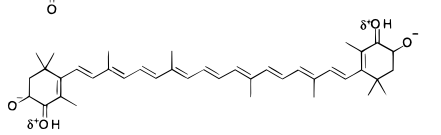	0	428[a] 425[b]
II	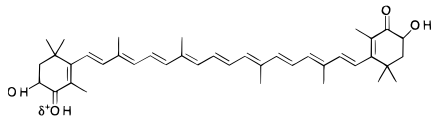	+1	718[a] 752[b]
III	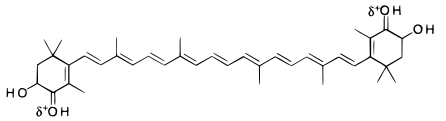	+2	609[a] 644[b]
IV	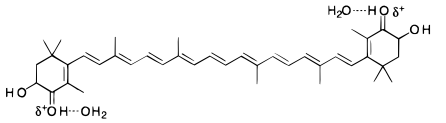	+2	608[b]
V	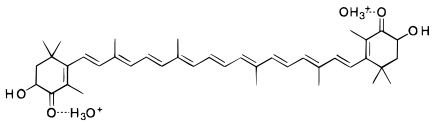	0/+2	470[a]
VI	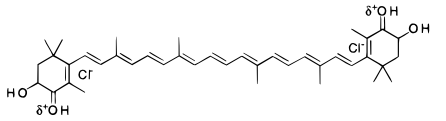	+2/-2	462[b]
VII	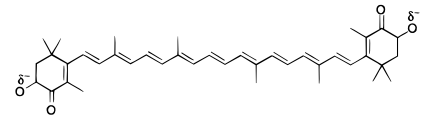	–2	396[a]
VIII	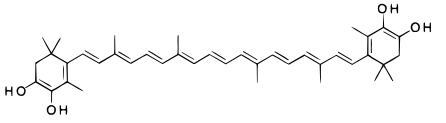	0	451[b]
IX	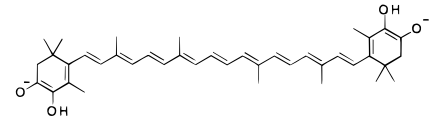	–2	710[b]

[a] AM1 parametrization. [b] PM3 parametrization. [c] For the doubly protonated form, which gives the closest match to the experimental data, refined models are presented, involving interaction with H_3O^+ ions instead of protonation or stabilization by water molecules or monovalent Cl^- counterions.

close to the ring (structure **VI**). Alternatively, a H_3O^+ ion can be placed in a hydrogen bonding configuration with the keto groups (structure **V**). Finally, the dienol and dienolate forms were considered (structures **VIII** and **IX**). These may represent resonance structures worth considering.

To arrive at a reliable theoretical evaluation of the λ_{max} for the various models, excited state energies were calculated with AM1 or PM3 in a configuration interaction calculation that included all singly excited configurations from the nine highest occupied orbitals to the nine lowest unoccupied orbitals. For astaxanthin, the homo−lumo electronic energy transition had the largest oscillator strength in the calculated electronic spectrum and corresponds with the λ_{max}, calculated at 441 and 432 nm for AM1 and PM3, respectively. This is close to the experimental absorption maximum λ_{max} of ∼480 nm. In general, transition energies depend on the electronic polarizability of the surrounding medium. Since solvent−carotenoid interactions are not included in the semiempirical modeling procedure, the calculated values should be lower than the experimental data. This justifies a comparison between the calculated excited state energies of model structures and the λ_{max} of α-crustacyanin, which can be used to exclude or favor certain mechanisms that could be responsible for the color shift upon going from free to protein-bound astaxanthin.

Establishing a red shift of 5000 cm^{-1} for the $\pi-\pi^*$ transition of the polyene chain in a single carotenoid apparently requires quite a strong additional charge polarization of the conjugated system, or even a positively charged molecule, e.g. by protonation of one or both of the keto groups. For positively charged structures **II**−**IV**, the calculated delocalization of the additional charge at the keto groups extends all the way into the chain and affects carbons up to C-15,15′ in the center of the molecule! This is achieved neither via internal hydrogen migration, from the hydroxy to the keto groups (structure **I**), nor in the dienol form (structure **VIII**). With negative charging, via deprotonation or in the dienolate form (structures **VII** and **IX**), the predicted shift effects would be of opposite sign. In the models presented in Table 2, 6-*s*-*cis* ring conformations were assumed, since these are most common in the crystal structures of carotenoids and retinoids (Hamanaka & Mitsui, 1972; Sterling, 1964; Bart & MacGillavry, 1968a,b). Due to the out-of-plane conformation of the *β*-rings with respect to the polyene chain, the conjugation of the carbon atoms in the ring is disturbed. The dihedral angles (5, 6, 7, and 8 and 5′, 6′, 7′, and 8′) calculated by AM1 and PM3 methods are close to 53°. However, changing the conformation of the rings from 6-*s*-*cis* to 6-*s*-*trans* would shift λ_{max} only by approximately 400 cm^{-1}, considerably less than the experimental value of 5000 cm^{-1} for the carotenoid in the protein.

During our explorations with the semiempirical quantum chemical methods, we did not find any other way to invoke color shifts of a similar magnitude accompanied by charge polarizations originating from the rings and affecting the entire polyene chain in a single astaxanthin molecule. In this respect, the conclusion from the Raman data that the carotenoids in the α-crustacyanin are spectroscopically monomeric represents a severe constraint.

DISCUSSION

The first stage of a ^{13}C CP/MAS NMR study on α-crustacyanin yielded information about the astaxanthin binding site by comparing the ^{13}C chemical shift of free astaxanthin with the corresponding chemical shift of astaxanthin bound to the α-crustacyanin complex (Weesie et al., 1995). In this way, an electrostatic effect of the protein environment on the central part at carbon positions 14,14′ and 15,15′ in the astaxanthin molecule was discovered. The incorporation and CP/MAS NMR of [12,12′-$^{13}C_2$]- and [13,13′-$^{13}C_2$]astaxanthin provide additional information about the charge effects in the central part of the chromophore.

Reconstitution studies involving α-crustacyanin and a range of natural and synthetic carotenoids have shown that the two keto groups at C-4 and C-4′ play a crucial role for binding and oligomerization to α-crustacyanin with its full

bathochromic shift (Warburton, 1986; Britton et al., 1997). In addition, the keto groups in the analogues must be conjugated with the polyene chain to form spectrally shifted complexes (Britton et al., 1997). Also, the presence of the two central methyl groups of the polyene chain at C-20 and C-20′ is critical, since neither 20,20′-dinorastacene, with the two central methyl groups of the polyene chain absent, nor 20-norastaxanthin, with only one central methyl group lacking, bound to the apoprotein to give blue complexes (Warburton, 1986). To probe these two important binding features and to provide additional insight into the origin of the asymmetry of the ligand−protein interactions, the ^{13}C CP/MAS NMR spectra of α-crustacyanin reconstituted with astaxanthins specifically ^{13}C-labeled at position 4,4′ or 20,20′ would be expected to be useful.

Astaxanthin in α-Crustacyanin Is Electrostatically Polarized. By comparison of the isotropic chemical shifts and band shapes of the ^{13}C resonance signals for the complexed and uncomplexed forms of astaxanthin, information can be obtained about the binding interactions of the astaxanthin−chromophore in the crustacyanin complex. For instance, the labels in the pure solid [12,12′-$^{13}C_2$]astaxanthin resonate with a σ_i of 140.2 ppm, while for the complex, two signals are observed, with σ_i values of 145.1 and 147.2 ppm, corresponding to downfield shifts $\Delta\sigma_i$ of 4.9 and 7.0 ppm, respectively (Table 1). This is again consistent with an electronic perturbation of the astaxanthin chromophore caused by binding, leading to a decrease in electronic charge density at both the C-12 and C-12′ positions in the middle part of the polyene chain.

A change in charge density of 1 electronic equivalent corresponds to a carbon chemical shift of approximately 155 ppm in aromatic and conjugated systems (Spiesecke & Schneider, 1968; Tokuhiro & Fraenkel, 1969; Strub et al., 1983). The 4.9 and 7.0 ppm downfield shifts of the 12,12′-$^{13}C_2$ resonances after binding to the α-crustacyanin complex can therefore be translated into 0.032 and 0.045 electronic equivalent of charge, respectively. This provides additional evidence that a charge redistribution mechanism contributes to the bathochromic shift of astaxanthin in α-crustacyanin. In addition, the $\Delta\sigma_i$ values for the 12,12′ compound are on the same order of magnitude as the 3.9 and 6.8 ppm shifts previously observed for [14,14′-$^{13}C_2$]astaxanthin, which can be translated into 0.025 and 0.044 electronic equivalent of charge, respectively (Weesie et al., 1995). The uncertainty in the values is determined by the intrinsic inaccuracy of the chemical shift versus charge correlation and can be as high as 20%.

The modest upfield shift of 1.9 ppm for the 13,13′-$^{13}C_2$ resonance signals is consistent with a small net increase in the electronic charge density at positions 13 and 13′ due to protein binding, in contrast to the decrease in electronic charge density at the C-14,14′ and C-12,12′ positions of the polyene chain. This parallels the case of [15,15′-$^{13}C_2$]-astaxanthin reported previously (Weesie et al., 1995). There the shift is in the same direction as that with the C-13,13′ resonance signals but is even smaller, from 130.1 ppm for the free form to 129.5 ppm for the astaxanthin in the complex. The observed shifts would translate into an increase of 0.012 and 0.004 electronic equivalent of charge for [13,13′-$^{13}C_2$]- and [15,15′-$^{13}C_2$]astaxanthin, respectively.

The ^{13}C responses of [4,4′-$^{13}C_2$]astaxanthin in α-crustacyanin are downshifted by 2.4 ppm. In this case, the chemical shift-electronic charge correlation may have to be applied with caution, since it was originally established for olefinic and aromatic carbons. Nevertheless, a shift of 2.4 ppm is small, and the corresponding charge effects should also be small, considering that the stabilization of positive charge at the keto carbons due to the presence of the strongly electronegative oxygen puts the keto ^{13}C response at a σ_i of ∼200 ppm, approximately 70 ppm downfield from the typical value for a neutral double bond, ∼130 ppm.

The shift of the resonance signal for [20,20′-$^{13}C_2$]astaxanthin upon complexation is only 0.4 ppm. In general, ^{13}C shifts of methyl substituents on polyenes are not very sensitive to changes in electronic charge density in the conjugated system. Changes in methyl carbon ^{13}C chemical shifts are, for instance, caused by gross structural perturbations or by steric hindrance. Thus, a mechanism for the bathochromic shift involving significant changes in the geometry of the central part of the chromophore originating at the methyl groups is not very likely, which corroborates the conclusion reached by Salares et al. (1979), who found that the central part of the chromophore is essentially unperturbed by the surrounding structure.

Unequal Binding of Astaxanthin in the α-Crustacyanin Complex. In our experiments, the astaxanthin molecules are labeled symmetrically. Although there are differences between the various monomers in the hexadecameric complex (Quarmby et al., 1977; Zagalsky, 1982), it is generally thought that the variations of the ligand−protein interactions are minor, since all optical experiments performed thus far have confirmed that there is only one single astaxanthin species in the complex [see e.g. Salares et al. (1979)]. In contrast, the 14,14′ labels exhibit different shifts upon complexation, leading to two signal components for the isotope labels in the α-crustacyanin complex (Weesie et al., 1995). This led us to conclude that the labels in the two halves of the molecule are inequivalent in the protein and give rise to two distinguishable signals (Weesie et al., 1995). The splitting of the 12,12′-^{13}C resonance signals corroborates the previous findings and provides additional support for the perturbation of the symmetry of the molecule proposed previously on the basis of the data of α-crustacyanin reconstituted with [14,14′-$^{13}C_2$]astaxanthin. For the 13, 13′, 15, and 15′ positions, the putative asymmetry of the binding site is masked because of the small shifts, which make it impossible to distinguish two separate ^{13}C resonance signals within both pairs.

Although an asymmetry is observed in the resonance signals at the 12,12′ and 14,14′ positions, the sign and order of magnitude of the $\Delta\sigma_i$ for both halves of the astaxanthin molecule are the same. On the scale of the CP/MAS NMR, the main perturbation of the astaxanthin chromophore upon binding to the protein in fact has a symmetric character, with similar effects on both halves of the astaxanthin molecule, while an additional smaller perturbation is responsible for the observed asymmetry. This is important since structural models for the monomer have been presented which have one end of the carotenoid capped by the protein and positioned in a strictly apolar and aprotic environment, with the other end exposed to the polar solvent (Keen et al., 1991a,b). Two of these monomeric units combine to give a capsule-like *β*-crustacyanin structure enclosing the two astaxanthin molecules. This particular configuration suggests a predominant asymmetry of the protein−chromophore interactions, in contrast with the NMR results, which suggest that the primary perturbation has a symmetric character,

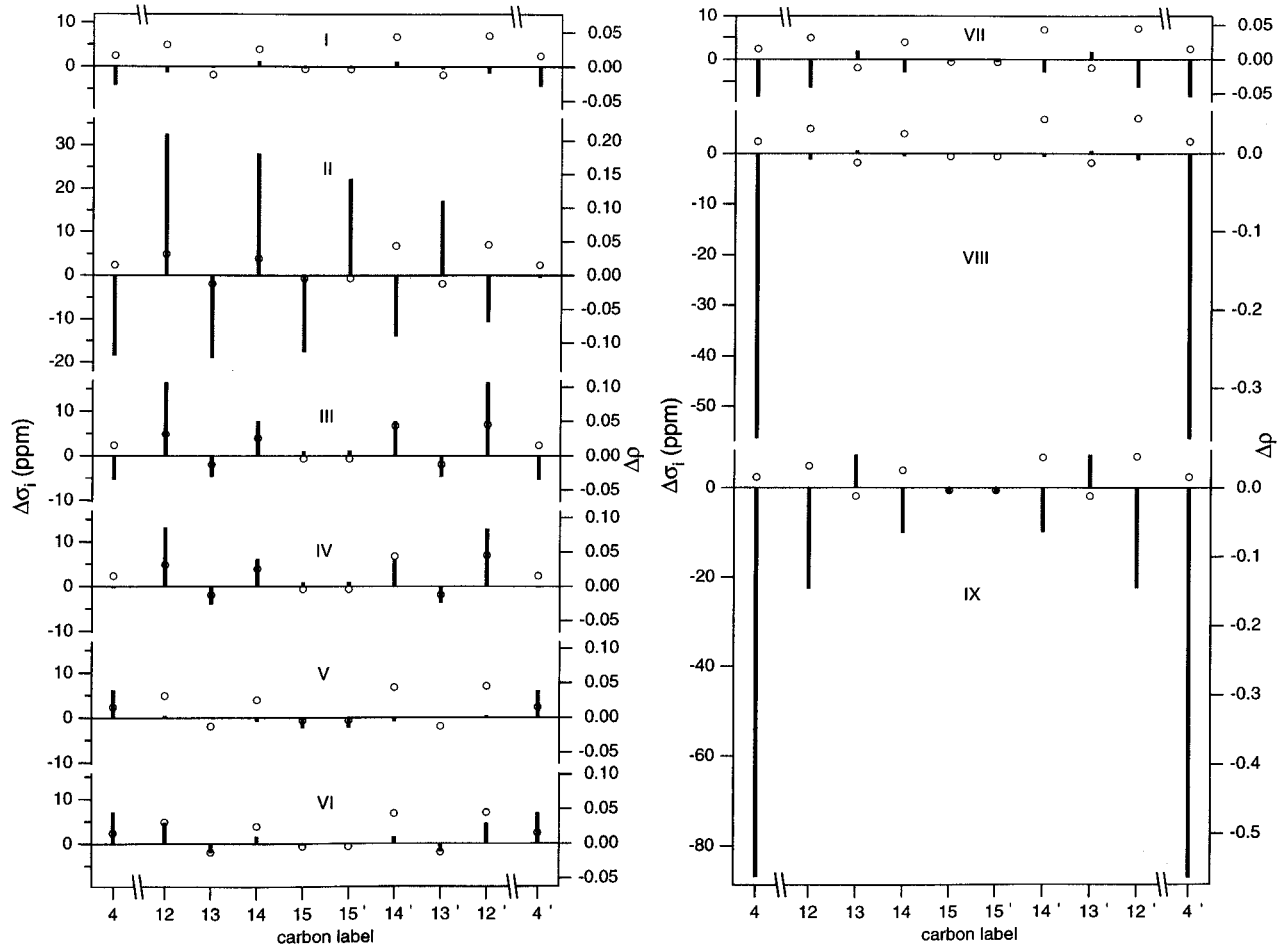

FIGURE 3: Chemical shift differences $\Delta\sigma_i$ between astaxanthin and α-crustacyanin (open circles), compared with calculated fractional electronic charge differences $\Delta\rho$ between astaxanthin and the set of model structures in Table 2 (bars). The ratio between the $\Delta\sigma_i$ and the $\Delta\rho$ axes amounts to 155 ppm per electronic charge equivalent.

originating from the keto groups (see below). This would require a protic environment and possibly charged amino acid residues in close proximity to both C-4 keto groups to bring about a protonation, which is not consistent with the structural model.

A Straightforward Charge Polarization Model for the Mechanism of the Bathochromic Shift. From the relatively small $\Delta\sigma_i$ for olefinic carbons in the central part, and also from the small $\Delta\sigma_i$ for the [20,20′-$^{13}C_2$]astaxanthin in the complex, it is now evident that the driving force behind a charge polarization mechanism associated with the bathochromic shift cannot be solely attributed to highly localized and specific interactions between the protein and the central part of the conjugated chain or the methyl groups. The main perturbation must then involve localized and specific interactions affecting the astaxanthin molecule outside the central region, most probably at the 4,4′-keto groups, since it is known that these are crucial for both binding and oligomerization to α-crustacyanin (Warburton, 1986; Britton et al., 1997). In addition, it also became clear in the quantum chemical modeling process that, if a pronounced electrostatic polarization or protonation of astaxanthin is involved in the color shift, it is most likely to originate from the keto groups in the β-rings. This was inferred from energy minimizations of a system in which a hydroxonium ion was placed in the direct vicinity of the astaxanthin molecule. When one ion is initially positioned in the direct neighborhood of the keto group in one β-ring, a proton can migrate toward the oxygen atom to form a protonated keto group stabilized by a hydrogen-bonded water molecule ($H_2O\cdots H-O{=}C = 2.060$ Å). The calculated heat of formation of the biprotonated complex ($\Delta H \cong 106.43$ kcal·mol^{-1}) is lower than that obtained for two hydroxonium ions hydrogen bonded ($OH_3^+\cdots O{=}C = 2.065$ Å) to the oxygen atoms ($\Delta H = 128.45$ kcal·mol^{-1}). This may be taken as an indication of a strong preference for interaction via the keto groups of the astaxanthin molecule. In addition, from these semiempirical modeling studies, it can be inferred that an interaction of the chain with an ionic species in or attached to the protein is not the most likely primary cause of the bathochromic shift.

On the other hand, the complexation shifts for the 4,4′-$^{13}C_2$ responses are small, and considerably smaller than those for the 12, 12′, 14, and 14′ responses, which may seem contradictory at first sight. In this light, modeling of electronic charge density profiles will help in investigating if strong interactions originating from the keto groups could, in principle, give rise to polarizations extending all along the chain up to the center of the molecule, while leaving the 4,4′ response virtually unaffected. In addition, the experimentally determined difference between the charge density profiles can be compared with the charge density variations calculated semiempirically.

Correlation of calculated charge densities with experimental chemical shift data is most effective when the differences $\Delta\sigma_i$ between two closely related compounds are considered rather than the absolute values [see e.g. Rodman-Gilson and Honig (1988)]. In Figure 3, the $\Delta\sigma_i$ values are

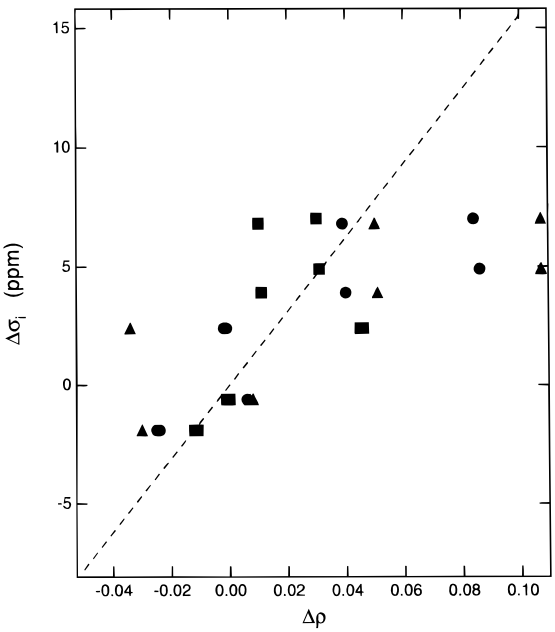

FIGURE 4: Chemical shift differences $\Delta\sigma_i$ versus fractional charge differences $\Delta\rho$ for the doubly charged model structures: (▲) the free structure **III**, (●) the structure **IV** stabilized with water molecules, and (■) the structure **VI** stabilized by monovalent Cl^- counterions. The dashed line indicates the Spiesecke−Schneider proportionality relation with a 155 ppm shift per unit of charge (Spiesecke & Schneider, 1961).

compared with the calculated electronic charge density differences $\Delta\rho$ for several forms of astaxanthin, in order to gain some insight into the nature of the protein binding and the mechanism of the bathochromic shift in α-crustacyanin. The assignment of the $\Delta\sigma_i$ values to symmetry-related positions on the two halves of the molecule is tentative. The scaling ratio between the left and right axes is 155 ppm per electron, allowing a direct comparison between the experimental $\Delta\sigma_i$ and the calculated $\Delta\rho$.

The models carrying the two positive charges generated by the protonation of the keto groups (structures **III**, **IV**, and **VI**) are the ones for which the signs of the $\Delta\rho$ and their orders of magnitude are in agreement with the experimentally determined $\Delta\sigma_i$, in the sense that there is a fair correlation with the Spiesecke−Scheider relation between shift and atomic charge densities (Figure 4). While it is obvious that further studies with astaxanthins labeled with ^{13}C will be required for a further characterization of the protein-chromophore interactions, it is still interesting that the calculated ^{13}C chemical shifts represent the right trend and support a newly developed class of hypothetical models for protein-bound astaxanthin. The best overall agreement, in terms of color and shift, is observed for structure **IV**. A mechanism involving charging and stabilization by H_2O is of particular interest, since reversible changes in color and NMR shifts have been reported upon dehydration and rehydration of the complex (Weesie et al., 1997). A water molecule in a complex counterion may thus be considered a likely candidate for driving the protonation process, as in e.g. retinal proteins (de Groot et al., 1990).

Regarding the other structures, for the dienol and the dienolate forms, large upfield shifts for the keto carbons are expected while the signs of the reconstitution shifts are opposite of the experimental values. Structure **II**, with the astaxanthin protonated at one keto group, can be rejected, since charge density differences are quite large in the center of the molecule and only match the signs of the $\Delta\sigma_i$ values in one half of the molecule. Also, the doubly deprotonated astaxanthin (structure **VII**) does not represent a valid model, since the calculated charge density differences exhibit the opposite signs or upfield−downfield pattern when compared with the experimental $\Delta\sigma_i$. Finally, a model in which a hydrogen atom has migrated from the hydroxyl groups to the keto groups in both β-rings (structure **I**) can be rejected. The effects on the charge density differences for the 4 and 4′ positions are large, and the effects in the part of the chromophore between C-13 and C-12′ are almost negligible. This contradicts the NMR data.

Additional support for a double charging or bisymmetrical polarization mechanism by e.g. a double protonation comes from the calculations of the λ_{max} for the different forms of astaxanthin (cf. Table 2). It has been pointed out that the absorption spectrum of a linear polyene shifts to lower energy in a solvent of increasing refractive index (Hudson et al., 1982; Hudson & Kohler, 1973), and variations of λ_{max} up to 40 nm are found for astaxanthin in different solvents (Buchwald & Jencks, 1968a). Therefore, the calculated λ_{max} for astaxanthin is in line with the experimental value of ∼480 nm. Of the models presented in Table 2, the double positively charged astaxanthins (structures **III** and **IV**) have the theoretical λ_{max} within 40 nm of the range of experimental values and may thus serve as possible candidates for the model of protein-bound astaxanthin. For structure **III**, the λ_{max} is calculated at 609 and 644 nm for AM1 and PM3, respectively, which is remarkably close to the absorption maximum of 632 nm for α-crustacyanin when the deviation of the isolated molecule to a shorter wavelength is taken into account. Additional features that either increase λ_{max}, like 6-*s*-*cis* to 6-*s*-*trans* configurational changes involving either one or both rings, or decrease λ_{max}, like the presence of counterions in the vicinity of the keto groups (structure **VI**), could also be additional influences on the red shift in the α-crustacyanin complex. In line with the NMR results, the quantum chemical calculations appear to reject a structure in which astaxanthin is only protonated at one keto group or the dienolate form (structures **II** and **IX**), since the calculated λ_{max} is too high. Likewise, astaxanthin that is deprotonated at the hydroxyl groups in both rings (structure **VII**), as well as the dienol form (structure **VIII**) or astaxanthin in which the hydrogens have migrated from the hydroxyl groups to the keto groups (structure **I**), has electronic absorption maxima that are too low.

A closer comparison between the calculated $\Delta\rho$ of the doubly protonated astaxanthin and the experimental $\Delta\sigma_i$ suggests that the $\Delta\rho$ values are overestimated, since the $\Delta\rho$ values for the 12,12′ positions translate into 12 ppm, exceeding the experimental $\Delta\sigma_i$ of 7.0 and 4.9 ppm (cf. Figure 3). However, calculations which included the presence of two Cl^- counterions symmetrically positioned at a distance of ∼3 Å from the protonated keto groups (structure **VI**) showed that this overestimation can easily be compensated for, although this stabilization mechanism also increases the electronic energy gap. It is possible, by varying the distance, to tune the values and dampen the effect of the protonated keto groups on the charge density distribution in the chromophore. On the other hand, the presence of counterions also affects the λ_{max} and reduces the red shift.

It must be emphasized that the strong and symmetric charge polarization model we propose here should be considered as a first step in refining and resolving the

ligand−protein interactions that are responsible for the color shift. Additional molecular mechanisms contributing to the red shift may have to be invoked when more experimental data are available in the future.

CONCLUSIONS

The results of the ^{13}C CP/MAS NMR experiments on α-crustacyanins reconstituted with specifically ^{13}C-labeled astaxanthins at the central positions (4,4′, 12,12′, 13,13′, 14,14′, and 15,15′) in combination with the results of quantum mechanical semiempirical calculations can be reconciled with a simple charging mechanism for the bathochromic shift, in which interaction of the keto groups in the β-rings is induced upon binding to the protein. For spectroscopically monomeric astaxanthin, the binding shifts $\Delta\sigma_i$ and the λ_{max} are in qualitative agreement with the model structures **III** and **IV**. Hence, a refined hypothesis for the mechanism of the bathochromic shift of astaxanthin in α-crustacyanin, formulated in terms of a strong symmetric polarization originating from both keto groups, is emerging from the combination of CP/MAS NMR and semiempirical modeling studies. This points to a simple charge polarization model for the bathochromic shift involving a protonation or another interaction with a positive ionic species with a comparable magnitude with *both* keto groups in astaxanthin.

The delocalization of charge into a conjugated polyene is the result of a subtle interplay between molecular parameters, mainly the bond-stretching forces, the on-site and nearest-neighbor Coulomb interactions, and the nearest-neighbor transfer integrals. It is well known that restricted Hartree−Fock calculations of conjugated systems present overestimation of the bond alternation pattern and that correlations are not well treated. Moreover, the calculations for structures **III** and **IV** predict the largest $\Delta\rho$ closer to the protonated keto groups, in particular at carbons 6 and 8 (positive charge) and 5 (negative charge). When astaxanthins labeled at these positions can be synthesized in a sufficient amount for the NMR analyses, a further refinement of the models for the bathochromic shift will be possible.

ACKNOWLEDGMENT

We thank C. Erkelens for assistance with the NMR experiments.

REFERENCES

Bart, J. C. J., & MacGillavry, C. H. (1968a) *Acta Crystallogr. B 24*, 1569−1587.

Bart, J. C. J., & MacGillavry, C. H. (1968b) *Acta Crystallogr. B 24*, 1587−1606.

Britton, G., Weesie, R. J., Askin, D., Warburton, J. D., Gallardo-Guerrero, L., de Groot, H. J. M., Jansen, F. J. H. M., Lugtenburg, J., Cornard, J.-P., & Merlin, J.-C. (1997) *Pure Appl. Chem.* (in press).

Buchwald, M., & Jencks, W. P. (1968a) *Biochemistry 7*, 834−843.

Buchwald, M., & Jencks, W. P. (1968b) *Biochemistry 7*, 844−859.

de Groot, H. J. M., Copié, V., Smith, S. O., Allen, P. J., Winkel, C., Lugtenburg, J., Herzfeld, J., & Griffin, R. G. (1988) *J. Magn. Reson. 77*, 251−257.

de Groot, H. J. M., Harbison, G. S., Herzfeld, J., & Griffin, R. G. (1989) *Biochemistry 28*, 3346−3353.

de Groot, H. J. M., Smith, S. O., Courtin, J., Van den Berg, E., Winkel, C., Lugtenburg, J., Griffin, R. G., & Herzfeld, J. (1990) *Biochemistry 29*, 6873−6883.

Gajewski, J. J., & Gilbert, K. E. (1991) *The MMX Method, Cadcom International Package*, Gennevilliers, France.

Hamanaka, T., & Mitsui, T. (1972) *Acta Crystallogr. B 28*, 214−222.

Honig, B., Dinur, U., Nakanishi, K., Balogh-Nair, V., Gawinowicz, M. A., Arnaboldi, M., & Motto, M. G. (1979) *J. Am. Chem. Soc. 101*, 7084−7086.

Hudson, B. S., & Kohler, B. E. (1973) *J. Chem. Phys. 59*, 4984−5002.

Hudson, B. S., Kohler, B. E., & Schulten, K. (1982) in *Excited States* (Lim, E. C., Ed.) pp 66−73, Academic Press, New York.

Jansen, F. J. H. M., Kwestro, M., Schmitt, D., & Lugtenburg, J. (1994) *Recl. Trav. Chim. Pays-Bas 113*, 552−562.

Keen, J. N., Caceras, I., Eliopoulos, E. E., Zagalsky, P. F., & Findlay, J. B. C. (1991a) *Eur. J. Biochem. 197*, 407−417.

Keen, J. N., Caceras, I., Eliopoulos, E. E., Zagalsky, P. F., & Findlay, J. B. C. (1991b) *Eur. J. Biochem 202*, 31−40.

Merlin, J. C., & Delé-Dubois, M. L. (1986) *Comp. Biochem. Physiol. 1*, 97−103.

Quarmby, R., Norden, D. A., Zagalsky, P. F., Ceccaldi, H. J., & Daumas, R. (1977) *Comp. Biochem. Physiol. 56B*, 55−61.

Rodman-Gilson, H., & Honig, B. H. (1988) *J. Am. Chem. Soc. 110*, 1943−1950.

Salares, V. R., Young, N. M., Bernstein, H. J., & Carey, P. R. (1979) *Biochim. Biophys. Acta 576*, 176−191.

Smith, S. O., Palings, I., Miley, M. E., Courtin, J., de Groot, H. J. M., Lugtenburg, J., Mathies, R. A., & Griffin, R. G. (1990) *Biochemistry 29*, 8158−8164.

Spiesecke, J., & Schneider, W. G., (1961) *Tetrahedron Lett.*, 468−472.

Sterling, C. (1964) *Acta Crystallogr. 17*, 1224−1228.

Strub, H., Beeler, A. J., Grant, D. M., Michl, J., Cutts, P. W., & Zilm, K. (1983) *J. Am. Chem. Soc. 105*, 3333−3334.

Tokohiru, T., & Fraenkel, G. (1969) *J. Am. Chem. Soc. 91*, 5005−5013.

van Liemt, W. B. S., Boender, G. J., Gast, P., Hoff, A. J., Lugtenburg, J., & de Groot, H. J. M. (1995) *Biochemistry 34* (32), 10229−10236.

Warburton, J. (1986) Ph.D. Thesis, University of Liverpool, Liverpool, England.

Weesie, R. J., Askin, D., Jansen, F. J. H. M., de Groot, H. J. M., Lugtenburg, J., & Britton, G. (1995) *FEBS Lett. 362*, 34−38.

Weesie, R. J., Verel, R., Jansen, F. J., Britton, G., Lugtenburg, J., & de Groot, H. J. M. (1997) *Pure Appl. Chem.* (in press).

Zagalsky, P. F. (1982) *Comp. Biochem. Physiol. 73B*, 997−1000.

Zagalsky, P. F. (1985) *Methods Enzymol. 111B*, 216−247.

Zagalsky, P. F., Clark, R. J. H., & Fairclough, D. P. (1983) *Comp. Biochem. Physiol. 75B*, 169−170.

Zagalsky, P. F., Eliopoulos, E. E., & Findlay, J. B. C. (1990) *Comp. Biochem. Physiol. 97B* (1), 1−18.

BI9631982